Original Research Article

Synthesis, characterization, herbicidal activities and *in silico* studies of some highly functionalized Oxazolone derivatives

ABSTRACT

Oxazolones, commonly referred to as azlactones, represent a versatile class of five-membered heterocyclic compounds characterized by the presence of nitrogen and oxygen as heteroatoms. The biological activities of oxazolone are primarily associated with modifications at the C-2 and C-4 positions. These compounds have been widely investigated for their herbicidal properties, which arise from their ability to inhibit specific enzymes essential for plant growth and development, ultimately causing weed suppression and death. A series of highly functionalized oxazolone derivatives were synthesized and characterized using techniques such as ^{1}H NMR, ^{13}C NMR, elemental analysis, FT-IR, and mass spectrometry. Their herbicidal activities were assessed in vitro against sterilized seeds of *Raphanus sativus* at varying concentrations (*25, 50, 75*, and *100* µg/mL). The half-maximal inhibitory concentration (IC_{50}) values of the ligands were calculated, revealing significant pre-emergent herbicidal activity. The results demonstrated that the herbicidal performance of the oxazolone derivative was superior to its -nitro and -methoxy counterparts but less effective compared to the standard herbicide pendimethalin. Additionally, in silico studies were conducted using PROTOX-II software and the SwissADME predictor to evaluate toxicity and herbicide-likeness. The compounds exhibited promising results in both in vitro and in silico analyses, highlighting the potential for further modification and exploration of oxazolone derivatives as potent herbicides.

Keywords:synthesis, herbicidal activity, oxazolone derivatives, azolactone,Raphanus sativus.

1. INTRODUCTION

Heterocyclic chemistry is regarded as one of the most intricate and diverse branches of organic chemistry. This field has been rapidly advancing, driven by the extensive application of heterocyclic compounds in pharmaceuticals, agriculture, and various industries (**Jain et al. 2006)**. Among these, nitrogen-containing heterocycles are particularly significant due to their abundance in nucleic acids.

Azole compounds, a prominent class of heterocyclic compounds, have gained considerable attention in drug discovery. Their ability to easily interact with enzymes and receptors in organisms through noncovalent interactions makes them valuable as lead compounds for developing effective therapeutic agents. These compounds have been employed to combat bacterial, fungal, malarial, viral infections and other common infections, as well as to address cancer and inflammatory conditions, as

highlighted by **Devasia et al. (2022)**.Among azole compounds, oxazole or oxazolone is recognized as one of the most vital structural units.

Oxazolone, also known as azlactone, belongs to a class of five-membered heterocyclic compounds featuring nitrogen and oxygen as heteroatoms. The oxazolone ring plays a crucial role in drug discovery and development. Many well-known marketed drugs, including rilmenidine, furazolidone, nifurantoin, oxaprozin, and notably linezolid-effective against methicillin-resistant Staphylococcus aureus **(Canon et al., 2017)** are based on the oxazolone framework.The various biological activities of oxazolone are predominantly associated with its C-2 and C-4 positions. The oxazolone framework finds extensive use across various fields, including agriculture, pharmaceuticals, and the food industry, as well as in natural products, medicine, polymers, and several other domains. It serves as a crucial intermediate in synthesizing a diverse array of small chemical molecules, such as amino alcohols **(Aaglawe et al., 2003)**, amino acids **(Giovanni et al., 2021)**, thiamine **(Ismail, 1991)**, amides **(Park et al., 1998)**, peptides, and multifunctional compounds. Oxazolone derivatives exhibit significant biological activities, including antimicrobial, antitubercular, anti-inflammatory, anticancer, and anti-HIV properties **(Kushwaha & Kushwaha, 2021)**. They also demonstrate antiangiogenic effects **(Muhittin, 2018)**, anticonvulsant activity **(Ibrahim et al., 2018)**, sedative and cardiotonic activity **(Khan et al., 2006)**, antidiabetic activity **(Tikdari et al., 2008)**, insecticidal activity **(Eman et al., 2021)**, and antiulcer activity **(Marian, 2005)**. The oxazolone group serves as the core structure in various biologically active natural compounds **(Bansal & Halve, 2014)**. The herbicidal properties of oxazolone derivatives arise from their capacity to inhibit certain enzymes essential for plant growth and development, ultimately causing growth suppression and the death of weeds.

In this study, a series of oxazolone derivatives were synthesized and evaluated for their herbicidal properties. Furthermore, various in-silico analyses were conducted to investigate the characteristics properties and potential activities of the synthesized compounds.

2. EXPERIMENTAL

The chemicals employed were of analytical reagent grade, ensuring exceptional purity, and were used as they stood, free from the need for further purification. The reagents included Furfural (purity >99%, Merck), acetic anhydride (purity >99.5%, Merck), hippuric acid (purity >98%, Merck), L-proline (purity >99%, Molychem), 4-methoxybenzoyl chloride (purity >99%, Merck), 4-nitrobenzoyl chloride (purity >98%, Merck), hydrochloric acid (purity >99%, Merck), and glycine (purity >99%, Merck), NaOH (purity >99%, Merck). Absolute ethanol (Merck) was used as the reaction medium.

2.1.Synthesis of ligands

The synthesis was carried out using a conventional procedure. In a 100 mL round-bottom flask, furfural (10 mmol, 0.828 mL), acetic anhydride (10 mmol, 0.945 mL), and hippuric acid derivatives (precursor, 10 mmol) were combined. To this reaction mixture, a catalytic amount of L-proline (10 mol% dissolved in 5 mL ethanol) was added. The reaction was conducted under reflux at room temperature with continuous stirring using a magnetic stirrer. Reaction progress was monitored

through thin-layer chromatography (TLC). Upon completion of the reaction, the reaction mixture was cooled the round bottom flask in an ice bath to quench the reaction. The resulting precipitate was collected by filtration, and the crude product was purified through recrystallization using a 1:3 mixture of acetone and ethanol respectively, yielding the final product **(Bhandari, 2018)**.

The crude product (4Z)-4-((furan-2-yl) methylene)-2-phenyloxazol-5(4H)-one (OD) underwent further purification through recrystallization. The same procedure outlined above was carried out for other derivatives, utilizing different reagents. Specifically, p-methoxyhippuric acid (yielding product (4Z)-4-((furan-2-yl) methylene)-4,5-dihydro-2-(4-methoxyphenyl) oxazole(MHA)) and p-nitrohippuric acid (yielding product (4Z)-4-((furan-2-yl) methylene-4,5-dihydro-2-(4-nitrophenyl) oxazole(NHA)) were used as substitutes for hippuric acid. The target synthesis products are depicted in **Schemes 1-3**.

The synthesis of oxazolone derivatives is depicted in **Schemes 1-3**, and their corresponding NMR spectral data are presented as follows:

$C_{14}H_9NO_3$ (OD) : ^{1}H NMR (400 MHz, DMSO-D6) δ(ppm): 6.37 (1H, dd, J = 3.4, 1.8 Hz), 7.12-7.28 (2H, 7.17 (s), 7.22 (dd, J = 3.4, 0.9 Hz)), 7.40-7.66 (3H, 7.47 (dddd, J = 7.6, 7.2, 1.7, 1.4 Hz), 7.59 (dddd, J = 7.9, 7.4, 1.3, 0.4 Hz)), 7.82 (1H, dd, J = 1.8, 0.9 Hz), 8.28 (2H, dtd, J = 7.9, 1.6, 0.4 Hz) ;^{13}C NMR (101 MHz, DMSO-D6) δ(ppm): 101.0 (1C, s), 112.0 (1C, s), 115.6 (1C, s), 126.7 (2C, s), 126.9 (1C, s), 127.8 (1C, s), 128.4 (2C, s), 142.6 (1C, s), 143.6 (1C, s), 152.1 (1C, s), 159.3 (1C, s), 166.2 (1C, s).

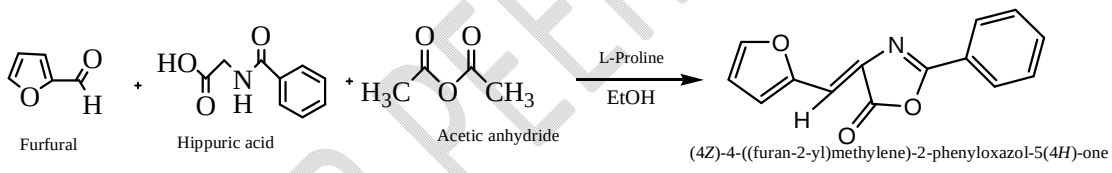

Furfural + Hippuric acid + Acetic anhydride → (4*Z*)-4-((furan-2-yl)methylene)-2-phenyloxazol-5(4*H*)-one

Scheme 1: Synthesis of (4Z)-4-((furan-2-yl) methylene)-2-phenyloxazol-5(4H)-one (OD).

$C_{15}H_{11}NO_4$ (MHA): ^{1}H NMR (400 MHz, DMSO-D6) δ(ppm):2.63 (2H, dd, J = 18.2, 6.1 Hz), 3.73 (3H, s), 4.99 (1H, dd, J = 8.1, 4.2 Hz), 6.22-6.37 (2H, 6.28 (dd, J = 3.4, 1.8 Hz), 6.32 (s)), 6.75-7.05 (4H, 6.81 (dd, J = 3.4, 0.8 Hz), 6.88 (ddd, J = 8.2, 2.9, 2.7 Hz), 6.95 (ddd, J = 2.9, 2.5, 0.5 Hz), 6.98 (ddd, J = 8.1, 2.7, 2.5 Hz)), 7.12-7.29 (2H, 7.17 (dd, J = 1.8, 0.8 Hz), 7.22 (ddd, J = 8.2, 8.1, 0.5 Hz)) ;^{13}C NMR (101 MHz, DMSO-D6) δ(ppm): 40.9 (1C, s), 55.5 (1C, s), 56.2 (1C, s), 104.6 (1C, s), 106.8 (1C, s), 110.3 (1C, s), 110.4 (1C, s), 113.1 (1C, s), 127.0 (1C, s), 129.4 (1C, s), 130.1 (1C, s), 137.8 (1C, s), 142.7 (1C, s), 152.5 (1C, s), 159.6 (1C, s), 207.5 (1C, s).

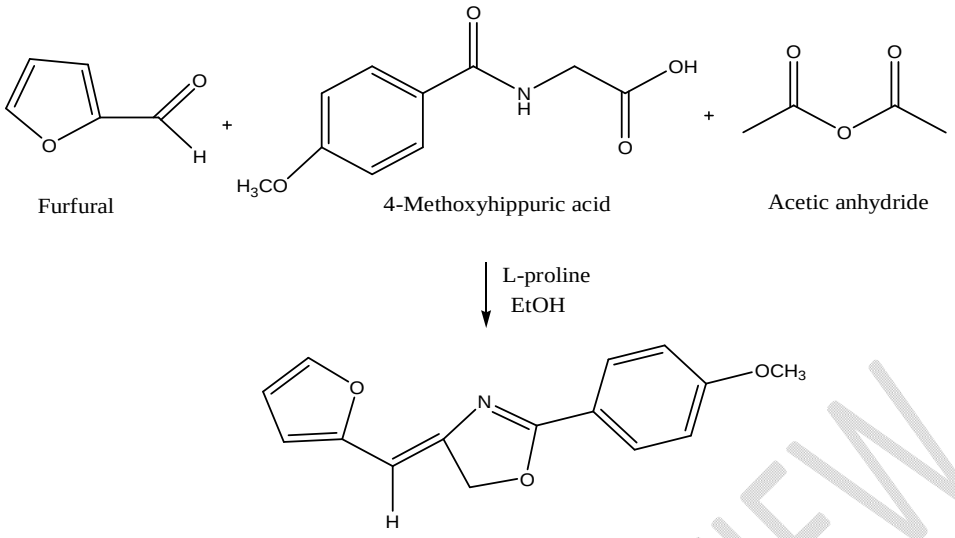

Scheme2: Synthesis of (4Z)-4-((furan-2-yl)methylene)-4,5-dihydro-2-(4-methoxyphenyl)oxazole (MHA).

$C_{14}H_9N_2O_5$ (NHA) : ^{1}H NMR (400 MHz, DMSO-D6) δ(ppm): 6.29 (1H, dd, J = 3.4, 1.8 Hz), 6.46-6.62 (2H, 6.51 (s), 6.57 (s)), 6.84 (1H, dd, J = 3.4, 0.8 Hz), 7.19 (1H, dd, J = 1.8, 0.8 Hz), 7.77 (2H, ddd, J = 8.6, 2.0, 0.5 Hz), 8.10 (2H, ddd, J = 8.6, 1.9, 0.5 Hz); ^{13}C NMR (101 MHz, DMSO-D6) δ(ppm): 71.1 (1C, s), 106.8 (1C, s), 110.3 (1C, s), 110.4 (1C, s), 123.7 (2C, s), 128.1 (2C, s), 130.1 (1C, s), 137.8 (1C, s), 142.7 (1C, s), 147.3 (1C, s), 152.5 (1C, s), 170.0 (1C, s).

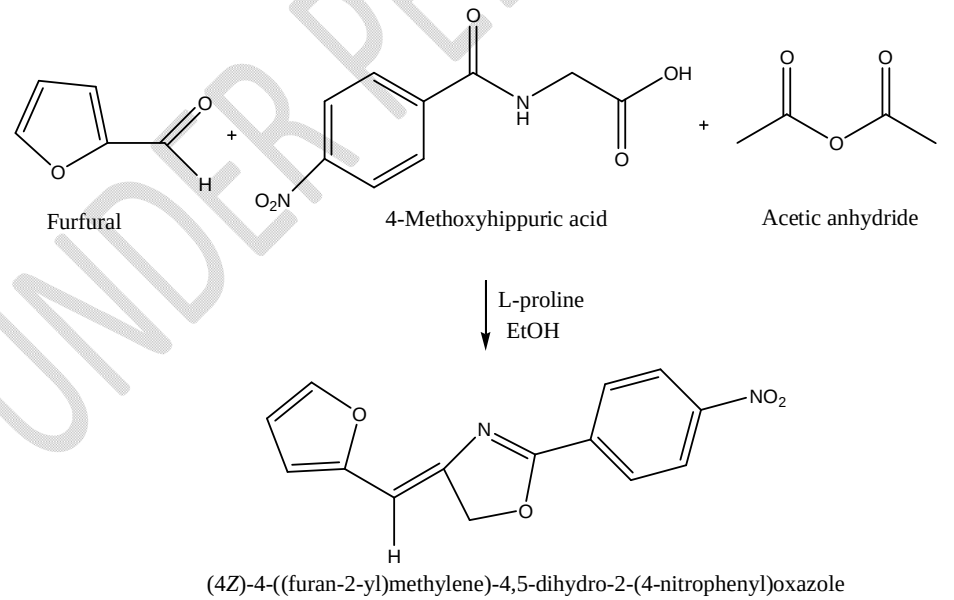

Scheme 3: Synthesis of (4Z)-4-((furan-2-yl) methylene-4,5-dihydro-2-(4-nitrophenyl) oxazole(NHA).

2.2Synthesis of precursor

Synthesis of Hippuric Acid Derivatives: Glycine (2 mmol) was dissolved in 100 mL of 10% sodium hydroxide solution (NaOH). Then, the appropriate benzoyl chloride derivatives, namely p-methoxybenzoyl chlorideand p-nitrobenzoyl chloride, were added portion-wise to the solution. The reaction mixture was stirred vigorously after each addition to ensure complete reaction of the chlorides, first for 1 hour at 5°C and then for another hour at room temperature. Subsequently, 2N hydrochloric acid solution (HCl) was added until the mixture became acidic, as indicated by litmus paper. The resulting precipitate of sufficient benzoyl glycine was filtered, washed multiple times with cold distilled water, dried, and crystallized **(Canan et al., 2017)**.

The formation of hippuric acid derivatives is depicted in **Schemes 4** and **5**, with their NMR spectral data provided as follows:

$C_{10}H_{11}NO_4$: ^{1}H NMR (400 MHz, DMSO-D6) δ(ppm): δ 3.72 (2H, s), 3.85 (3H, s), 7.08 (2H, ddd, *J* = 8.3, 1.1, 0.4 Hz), 8.00 (2H, ddd, *J* = 8.3, 1.8, 0.4 Hz);^{13}C NMR (101 MHz, DMSO-D6) δ(ppm): δ 41.1 (1C, s), 55.3 (1C, s), 113.9 (2C, s), 129.6 (1C, s), 130.0 (2C, s), 162.4 (1C, s), 166.3 (1C, s), 171.3 (1C, s).

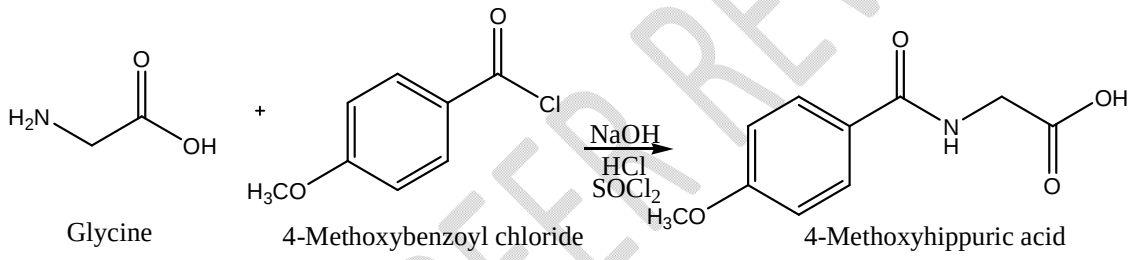

Scheme 4: Synthesis of p-Methoxy hippuric acid.

$C_9H_8N_2O_5$: ^{1}H NMR (400 MHz, DMSO-D6) δ(ppm):δ 3.74 (2H, s), 8.05-8.18 (4H, 8.12 (ddd, *J* = 8.6, 1.4, 0.5 Hz), 8.12 (ddd, *J* = 8.6, 1.8, 0.5 Hz));^{13}C NMR (101 MHz, DMSO-D6) δ(ppm):δ 41.1 (1C, s), 123.9 (2C, s), 128.2 (2C, s), 129.6 (1C, s), 149.4 (1C, s), 166.3 (1C, s), 171.3 (1C, s).

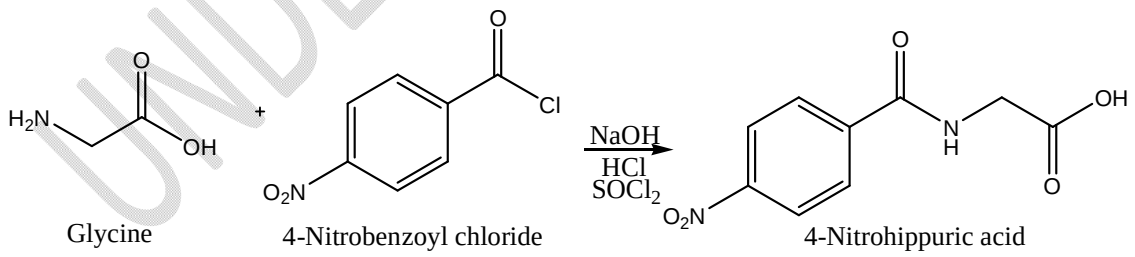

Scheme 5: Synthesis of p-Nitrohippuric acid.

2.3 Physical and Spectral Measurement

The melting point of the compound was determined with the Decibel DB-3135H melting point apparatus, while its molar conductivity was measured using the Systronic conductivity TDS meter 308. Elemental analysis for carbon (C), hydrogen (H), and nitrogen (N) was performed using the ElementarAnalysensysteme Germany (Vario Micro Cube). Magnetic molar susceptibilities were

evaluated at room temperature using Quincke's Tube and the Digital Gaussmeter (DGM-102). The molecular weight of the compound was determined via Mass Spectrometry with the Xevo G2-XS QT of Mass Spectrophotometer. ^{1}H-NMR and ^{13}C-NMR spectra were acquired using the Jeol JNM-ECZ 400S instrument (operating at frequencies of 400 MHz and 100 MHz, respectively), and FTIR analysis was conducted using the Nicolet iS50 FTIR Tri-detector.

2.4 Herbicidal Activity

The herbicidal activity of the synthesized compounds was assessed using a modified version of the method, where the compounds were dissolved in distilled water along with a 5% Tween-20 solution (**Vasilakoglou et al. 2013)**.

Bioassays using Petri dishes were performed to evaluate the impact of different extract components on the germination, root, and shoot growth of radish (*Raphanus sativus*) seeds. The seeds, obtained from Pantnagar, were went under sterilization with 95% ethanol for 15 seconds to eliminate potential contamination from bacteria or fungi. To assess the herbicidal potential of the extract, Petri dishes containing germination paper and 10 *Raphanus sativus* seeds, each were treated with 3mL of various concentrations (25, 50, 75, and 100 µg/mL) of extracted compounds. A 5% Tween-20 solution in distilled water was served as the negative control, while a Pendimethalin solution was used as the positive control. Each treatment was replicated three times with separate Petri dishes, and the experiment was carried out at a room temperature of 25-28°C. Five days post-treatment, the germination rate, root length, as well as shoot length were recorded. Seed inhibition and germination were monitored at 24, 48, 72, 96, and 120 hours post-treatment.

The percentage inhibition of germination for herbicidal activity was assessed using the following equation:

$$\% \textbf{ Inhibition } = \frac{\textbf{Germination in control - Germination sample}}{\textbf{Germination in control}} \times \mathbf{100}$$

2.5 ADMET and Toxicology Studies

Virtual screening was conducted to evaluate the physicochemical properties and examine the pharmacokinetics (drug-likeness) of selected compounds using the SwissADME tool **(Daina et al., 2017; Šestić et al., 2023)**. At the same time, the PROTOX-II software was used to assess oral toxicity and bioavailability **(Banerjee et al., 2018)**. ChemDraw software was employed to generate the required SMILES format for use in SwissADME and PROTOX-II **(Abdullahi & Adeniji 2020)**.

3. RESULTS AND DISCUSSION

3.1IR Spectral Data

The FT-IR spectra of the samples were recorded after complete dehydration in a hot air oven to remove any water molecule peaks, ensuring precise measurements. The corresponding spectral values are presented in **Table 1**.

Table 1: Corresponding values of FT-IR spectra.

Compound	v(N-H)	v(C=O)	v(C-N)	v(C=C)
OD	3335	~1648 (s)	~1213 (s)	900-1100
MHA	3381	1680 (sh)	1256 (sh)	900-1100
NHA	3348	~1685(s)	~1279 (s)	900-1100

All three compounds (OD, MHA, and NHA) exhibited N-H stretching around 3340 cm^{-1} and C=O stretching near 1680 cm^{-1}, indicating the presence of both amine and carbonyl groups in each, with only slight variations. These differences could be attributed to substitutions in the amine group, as observed by the C=C stretch at 1549 cm^{-1}, C=O stretch at 1752 cm^{-1}, and C-O-C stretch at 1023 cm^{-1} in MHA and NHA, respectively. Thus, the spectral analysis confirms the presence of both amine and ketone groups in all three samples. Furthermore, a C-NO_2 group is identified in NHA, while a C-OCH_3 group is found in MHA.

3.2 NMR Analysis

All the synthesized compounds exhibited a remarkable agreement with the expected ^{1}H and ^{13}C spectra. In the ^{13}C spectra, each compound displayed a carbonyl peak in the range of 160-170 ppm, corresponding to the carbonyl carbon of the oxazolone derivative. In the ^{1}H spectra, the peaks between 4.99-4.75 ppm and 3.49-3.73 ppm were attributed to the β and α carbons (adjacent to the carbonyl group), respectively. The values between 3.13-3.36 ppm corresponded to the N-H stretch. Thus, all the compounds were identified as oxazolone derivatives. Additionally, the chemical shift at 3.73 (s, 3H) is characteristic of the O-CH_3 bond, which was observed in MHA (a methoxy derivative).

3.3 UV-Vis Spectral Analysis

The UV-Vis spectra, along with the associated λ_{max} values provided in **Table 2**, show the formation of three distinct compounds. A redshift is observed as the size of the substituent group increases. **Table 2** also outlines the elemental composition, demonstrating a strong similarity between the calculated and experimental values.

Table 2: CHN Elemental Analysis data and UV-Vis Spectral values.

Compound	C	H	N	λ_{max}
OD	79.62 (83.69)	5.340 (6.35)	7.89 (4.65)	230
MHA	74.79 (75.11)	5.226 (5.4)	4.97 (4.17)	240

NHA	78.82 (79.73)	6.134 (6.39)	4.67 (4.236)	350

3.4 Herbicidal activity

Herbicidal activity and their half inhibition concentration (IC_{50}) was evaluated by measuring both the percentage inhibition of root germination and shoot germination across a concentration range of 25-100 ppm. Three separate analyses were conducted, including % seed germination (**Table 5**), % root inhibition (**Table 3**), and % shoot inhibition (**Table 4**). In all instances of root or shoot germination inhibition, it was noted that as the concentration of the compounds decreased, the % inhibition also decreased. The observed order of root inhibition, shoot inhibition and seed germination inhibition was as follows: Pendimethalin > MHA> OD> NHA.

Table 3: Percentage of root inhibition of Oxazolone derivatives.

HERBICIDAL ACTIVITY: Mean % ROOT INHIBITION						
S. No.	**Root Inhibition**	**100 ppm**	**75 ppm**	**50 ppm**	**25 ppm**	**IC_{50}**
1	**OD**	62.91	49.16	32.08	21.25	62.60
2	**MHA**	73.33	55.83	50.41	36.66	62.36
3	**NHA**	47.08	32.91	24.16	20.41	75.43
4	**Standard**	99.970	95.395	91.356	85.369	56.52

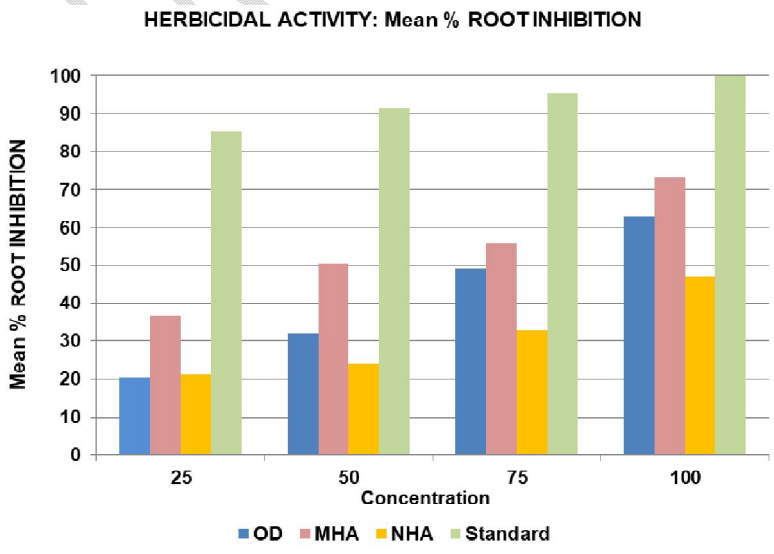

Fig. 1.Percentage root inhibition values of oxazolone derivative ligands at different concentrations.

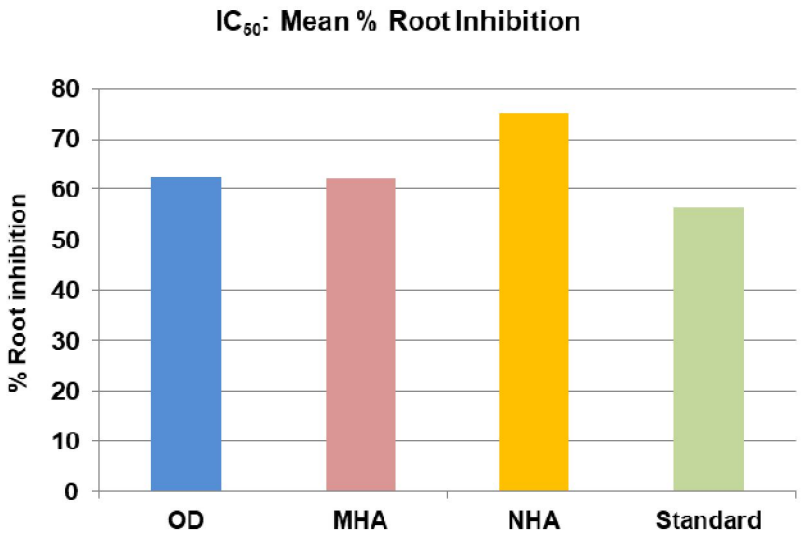

Fig. 2.IC_{50} values of percentage root inhibitionof oxazolone derivative ligands at different concentrations.

Table 4: Percentage shoot inhibition of Oxazolone derivatives.

HERBICIDAL ACTIVITY: % SHOOT INHIBITION						
SR No.	**Shoot Inhibition**	**100 ppm**	**75 ppm**	**50 ppm**	**25 ppm**	**IC_{50}**
1	**OD**	59.04	49.57	42.85	39.95	70.53
2	**MHA**	74.38	60.01	46.66	41.95	62.21
3	**NHA**	50.57	44.76	39.61	34.76	72.77
4	**Standard**	99.97	97.79	93.72	91.92	61.92

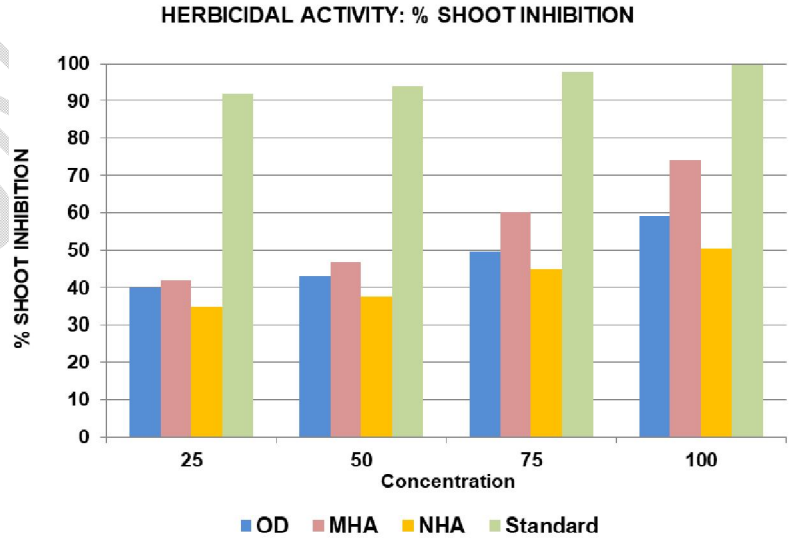

Fig. 3. Percentage shoot inhibition values of oxazolone derivative ligands at different concentrations.

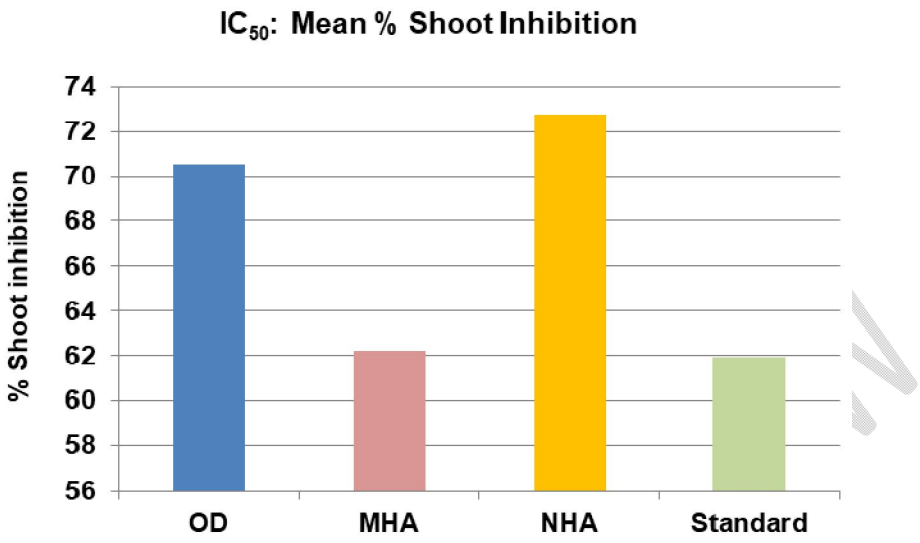

Fig. 4.IC_{50} values of percentage shoot inhibition of oxazolone derivative ligands at different concentrations.

Table 5: Percentage seed inhibition of Oxazolone derivatives.

S.No.	Compound	% inhibition seed germination activity				
		25 ppm	50 ppm	75 ppm	100 ppm	IC_{50}
1	OD	22.00±4.71	26.66±0.00	46.66±4.71	66.66±0.00	61.88
2	MHA	20.00±4.71	25.66±0.00	40.00±4.71	43.33±0.00	67.29
3	NHA	3.33±4.71	13.33±4.71	20.00±8.16	40.00±4.71	70.03
4	Standard	100	100	100	100	4.39

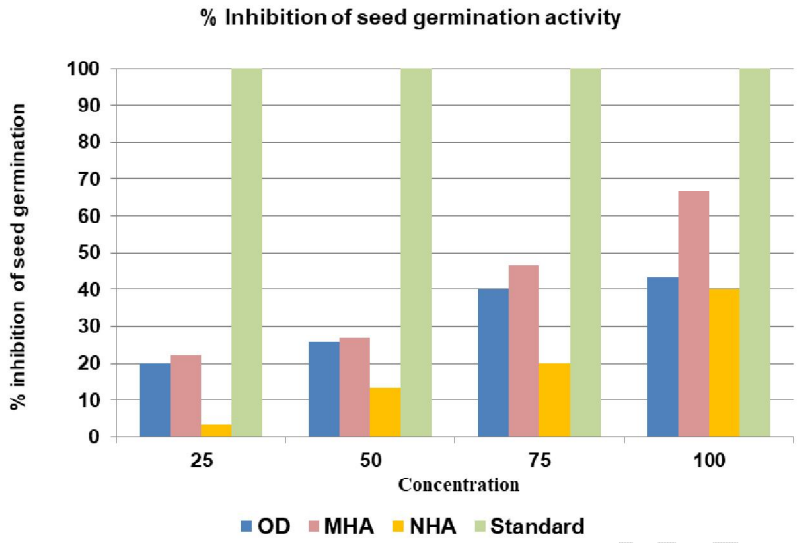

Fig. 5.Percentage inhibition of seed germination values of oxazolone derivative ligands at different concentrations.

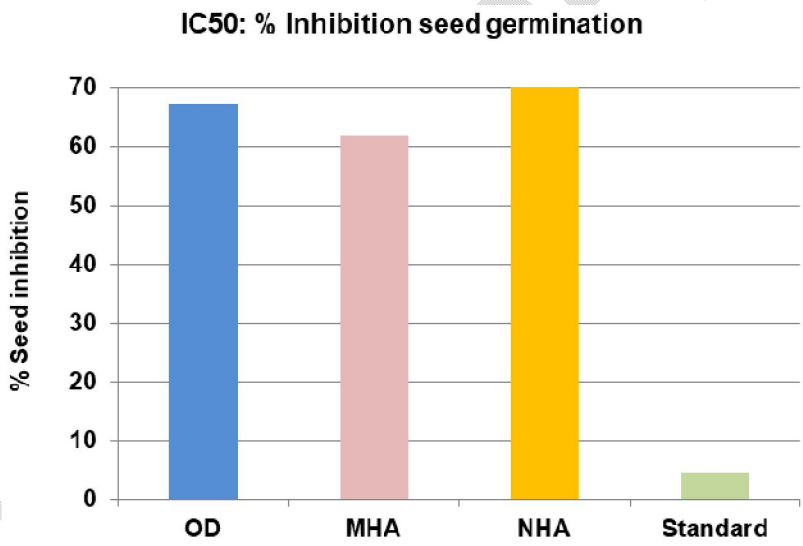

Fig. 6.IC_{50} values of percentage inhibition of seed germination of oxazolone derivative ligands at different concentrations.

3.5 ADMET and Toxicity Studies

The compounds were subjected to in-silico studies on Absorption, Distribution, Metabolism, Excretion (ADME), and toxicity. These computational analyses were used to predict and assess the pharmacokinetic characteristics and potential toxicity, offering valuable insights into the compounds' bioavailability and safety profiles, as shown in **Table 6**and **Fig. 7**. Additionally, the compounds were considered favorable in terms of drug-likeness, adhering to Lipinski's rule of five **(Nogara et al., 2015)**, highlighting their potential for effective pharmaceutical use.

Table 6: *in-silico* ADME and toxicity studies of the synthesized compounds.

Compound	M.wt.	H-bond donors	H-bond acceptors	Log P	Drug-Likeliness	LD_{50}	Toxicity Class
OD	**239.23**	0	3	2.06	Yes	3500	5
MHA	**269.30**	1	3	3.26	Yes	1016	4
NHA	**286.24**	1	4	3.23	Yes	1220	4

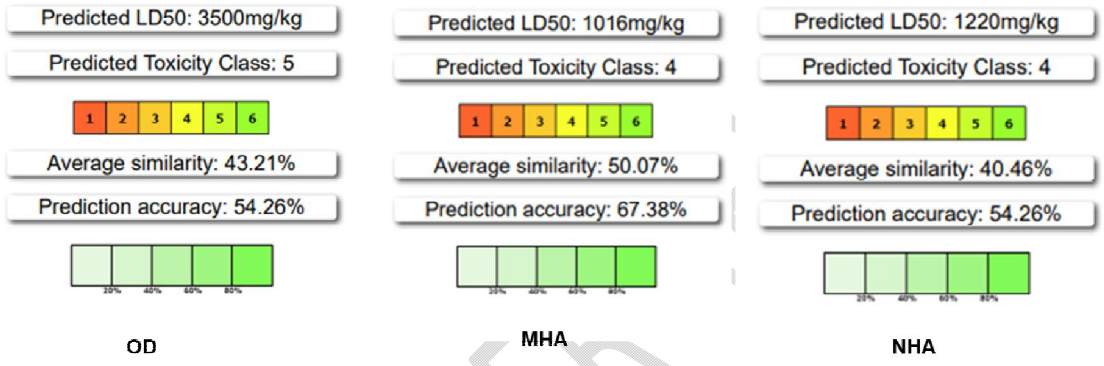

Fig. 7. in-silico ADME and toxicity studies of the synthesized compounds.

4. CONCLUSION

The synthesis of the oxazolone derivative (OD) and its -nitro (NHA) and -methoxy (MHA) derivatives was successfully achieved and characterized usingvarious spectroscopic and analytical methods. The herbicidal activity and their half inhibition concentration (IC_{50}) of OD, MHA, and NHA was evaluated on *Raphanus sativus* seeds at four different concentrations (100 µg/ml, 50 µg/ml, 75 µg/ml, and 25 µg/ml). Pendimethalin served as a positive control (standard), demonstrating the highest percentage inhibition of seed germination, while water was used as a negative control, showing the lowest inhibition. MHA exhibited the highest seed germination inhibition at the highest concentration, and the herbicidal activity followed this order: MHA > OD>NHA. For root and shoot inhibition, the observed order was: Pendimethalin > MHA > OD > NHA. A dose-dependent inhibition was noted for all three compounds, with minimal effects at lower concentrations and maximum effects at higher concentrations. SwissADME and PROTOX-II analyses revealed that the compounds exhibited low toxicity, with OD and NHA classified in toxicity class V and IV, respectively, and MHA in class IV, showing a higher LD_{50} value than the standard. Both in vitro and in silico studies indicated promising results, suggesting the potential for further modifications and exploration of oxazolone derivatives as effective herbicides.

REFERENCES

Aaglawe, M.J., Dhule, S.S., Bahekar, S.S., Wakte, P.S., & Shinde, D.B. (2003). Synthesis and antibacterial activity of some oxazolone derivatives. Journal of Korean Chemical Society, 47, 133-136.http://dx.doi.org/10.5012/jkcs.2003.47.2.133

Abdullahi, M., & Adeniji, S. E. (2020). In-silico molecular docking and ADME/pharmacokinetic prediction studies of some novel carboxamide derivatives as anti-tubercular agents. Chemistry Africa, 3(4), 989-1000.https://doi.org/10.1007/s42250-020-00162-3.

Banerjee, P., Eckert, A. O., Schrey, A. K., & Preissner, R. (2018). ProTox-II: a webserver for the prediction of toxicity of chemicals. Nucleic Acids Research, 46(W1), W257-W263.https://doi.org/10.1093/nar/gky318.

Bansal, S., & Halve, A. K. (2014). Oxazolines: Their synthesis and biological activity. International Journal of Pharmaceutical Sciences and Research, 5(11), 4601. 10.13040/IJPSR.0975-8232.5(11).4601-16.

Bhandari, S. (2018). Development of green methodologies for the synthesis of some biologically active heterocyclic and β-amino carbonyl compounds (Doctoral dissertation, GB Pant University of Agriculture and Technology, Pantnagar-263145 (Uttarakhand).http://krishikosh.egranth.ac.in/handle/1/5810093698.

Canan, K. U. Ş., Uğurlu, E., D ÖZDAMAR, E., & Benay, C. E. (2017). Synthesis and antioxidant properties of new oxazole-5 (4H)-one derivatives. Turkish Journal of Pharmaceutical Sciences, 14(2), 174.https://doi.org/10.4274/tjps.70299.

Daina, A., Michielin, O., & Zoete, V. (2017). SwissADME: a free web tool to evaluate pharmacokinetics, drug-likeness and medicinal chemistry friendliness of small molecules. Scientific reports, 7(1), 42717. https://doi.org/10.1038/srep42717.

Devasia, J., Nizam, A., & VL, V. (2022). Azole-based antibacterial agents: A review on multistep synthesis strategies and biology. Polycyclic Aromatic Compounds, 42(8), 5474-5495. https://doi.org/10.1080/10406638.2021.1938615.

Eman, A.G., Naglaa, F.H.M., & Eman, A.E.E. (2021).Syntheis, DFT and eco-friendly insecticidal activity of some Nheterocycles derived from 4-((2-oxo-1,2-dihydroquinolin-3-yl)methylene)-2-phenyloxazol-5(4H)- one.Bioorganic Chemistry, 112, 104945. https://doi.org/10.1016/j.bioorg.2021.104945.

Giovanni, P., Cinzia, T., Lara, B., Alice, B., Maria, M.C., Lara, S., Laura, Q., Annalisa, D.P., Leonardo, C., Antonia, R., & Giovanni, L. (2021). Densely Functionalized 2-Methylideneazetidine: Evaluation as Antibacterials. Molecules, 26, 3891-3908.https://doi.org/10.3390/molecules26133891.

Ibrahim, H.N., Daygu, B.C., Gul, Y., Derya, T., Muhittin, A., & Serap, A. (2018). Spectroscopic, Structural and Density Functional Theory (DFT) Studies of Two Oxazol-5-one Derivatives. Acta ChimicaSlovenica, 65, 86- 96.https://doi.org/10.17344/acsi.2017.3613.

Ismail, M.I. (1991). Physical characteristics and polarographic reduction mechanism of some oxazolones. Canadian Journal of Chemistry, 69, 1886-1892.https://doi.org/10.1139/v91-273.

Jain, A., Saxena, S., Rai, A. K., & Saxena, P. N. (2006). Assessment of toxicity of some penta-and hexacoordinated organotin (IV) and tetracoordinated tin (II) complexes of heterocyclic β-diketones. Bioinorganic Chemistry and Applications, *2006*.https://doi.org/10.1155/BCA/2006/60140.

Khan, K.M., Mughal, U.R., Khan, M.T.H., Ullah, Z., Perveen, S., & Choudhary, M.I. (2006) Oxazolones: new tyrosinase inhibitors; synthesis and their structure-activity relationships. Bioorganic & Medicinal Chemistry, 14, 6027–6033.https://doi.org/10.1016/j.bmc.2006.05.014.

Kushwaha, N., & Kushwaha, S. (2021). Synthetic approaches and biological significance of oxazolone moieties: A review. Biointerface Res. Appl. Chem, 12(5), 6460-6486.https://doi.org/10.1155/BCA/2006/60140.

Marian, P. (2005). Spectral characterization of oxazol-5(4H)-ones containing a furan and/or benzene ring in conjugation with the azlactone system. Journal of Chemical Research, 12, 766- 771.https://doi.org/10.3184/030823405775147031.

Muhittin, A. (2018). Structural characterization and DFT studies of an oxazol-5-one derivative. BalikesirUniversitesi Fen BilimleriEnstitusuDergisi, 20, 389-397.https://doi.org/10.25092/baunfbed.414333.

Nogara, P. A., Saraiva, R. D. A., Caeran Bueno, D., Lissner, L. J., Lenz Dalla Corte, C., Braga, M. M., & Rocha, J. B. T. (2015). Virtual screening of acetylcholinesterase inhibitors using the Lipinski's rule of five and ZINC databank. BioMed Research International, 2015. https://doi.org/10.1155/2015/870389.

Park, B.S., Min, Oh.C., Chun, K.H., & Lee, J.O. (1998). Photoinduced one pot transformation of 2- phenyl-4- ethylidene-5(4H)-oxazolone and allylic alcohols to γ, δ-unsaturated N-benzoyl

amides. Tetrahedron Letters, 39, 9711- 9714. https://doi.org/10.1016/S0040-4039(98)02232-1.

Šestić, T. L., Ajduković, J. J., Marinović, M. A., Petri, E. T., & Savić, M. P. (2023). In silico ADMET analysis of the A-, B-and D-modified androstane derivatives with potential anticancer effects. Steroids, 189, 109147. https://doi.org/10.1016/j.steroids.2022.109147.

Tikdari, A.M., Fozooni, S., &Hamidian, H. (2008).Dodecatungstophosphoric acid ($H_3PW_{12}O_{40}$), samarium and ruthenium (iii) chloride catalyzed synthesis of unsaturated 2-phenyl- 5(4H)-oxazolone derivatives under solvent-free conditions. Molecules, 13, 3246-3252. https://doi.org/10.3390/molecules13123246.

Vasilakoglou, I., Dhima, K., Paschalidis, K., &Ritzoulis, C. (2013). Herbicidal potential on Loliumrigidum of nineteen major essential oil components and their synergy. Journal of Essential Oil Research, 25(1), 1-10.https://doi.org/10.1080/10412905.2012.751054.